Supplementary appendix: *STK11* Mutations and PD-1 Inhibitor Resistance in *KRAS*-Mutant Lung Adenocarcinoma

Table of contents

Figure S1

A.

Characteristic	KL (N=54)	KP (N=56)	K-only (N=64)
Age at start of immunotherapy - yr			
Median	64	66	66
Range	48-86	42-81	52-87
Sex - no. of patients (%)			
Female	31 (57)	33 (59)	41 (64)
Male	23 (43)	23 (41)	23 (36)
Treatment center - no. (%)			
MDACC	11 (18)	23 (37)	28 (45)
MSKCC	22 (39)	15 (27)	19 (34)
DFCI/MGH	21 (38)	18 (32)	17 (30)
Smoking status - no. (%)			
Never smoker	2 (4)	3 (5)	8 (13)
Past/current smoker	49 (91)	51 (91)	54 (84)
Unknown	3 (6)	2 (4)	2 (3)
Immunotherapy agent - no. (%)			
Nivolumab	45 (83.3)	45 (80.5)	56 (87.5)
Pembrolizumab	4 (7.4)	8 (14.3)	7 (11)
Anti-PD-1/PD-L1 and anti-CTLA-4	5 (9.3)	3 (5.4)	1 (1.5)
Previous systemic therapies - no.			
Median	1	1	1
Range	0-5	0-5	0-6

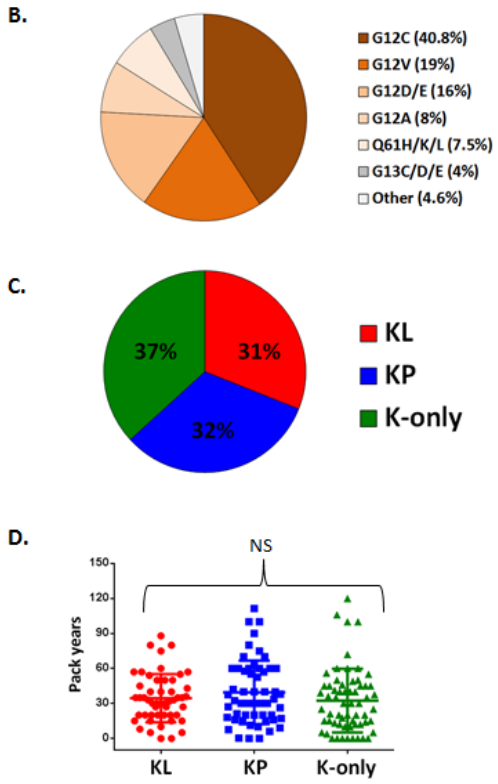

Figure S1. Demographic, clinical and molecular features of immunotherapy-treated patients with *KRAS*-mutant LUAC in the SU2C cohort (N=174). A. Baseline demographic and clinical characteristics of patients in the KL, KP and K-only subgroups. B. Pie chart representation of different *KRAS*-mutant alleles. C. Pie chart representation of co-mutation-defined subgroups of *KRAS*-mutant LUAC. Triple-mutant tumors (*KRAS;STK11/LKB1;TP53*) (13/174, 7.5%) were classified as KL based on previous work demonstrating shared transcriptional and immune profiles. D. Comparable smoking exposure, measured in pack-years, in the KL, KP and K-only subgroups (P=0.26, Kruskal-Wallis test).

Figure S2

ID	STK11 mutation	Functional Impact (FI)	FI score (Mutation Assessor)	Polyphen-2	Polyphen-2 score	BOR
MDACC1	p.D277fs*8	High				PD
MDACC2	p.L183P	High	3.86	Probably damaging	1	PR
MDACC3	p.Q37*	High				PD
MDACC4	p.G242V	High	4.69	Probably damaging	1	PD
MDACC5	p.Y60*	High				PD
MDACC6	c.465-2A>T	High				PD
MDACC7	p.H168P	High	4.17	Probably damaging	1	PD
MDACC8	p.N266fs	High				PD
MDACC9	p.G163R	High	3.85	Probably damaging	1	PD
MDACC10	p.K287*	High				PD
MDACC11	exon 1 deletion	High				SD
MSKCC1	p.K96X	High				PD
MSKCC2	p.E165*	High				SD
MSKCC3	exon 5 splice variant	High				PR
MSKCC4	p.N181S	High	3.53	Probably damaging	1	PD
MSKCC5	p.R304W	Low	1.54	Probably damaging	1	PD
MSKCC6	p.E57fs	High				PD
MSKCC7	exon 2 splice variant	High				PD
MSKCC8	exon 1 splice variant	High				PD
MSKCC9	p.C132fs	High				PD
MSKCC10	p.A43fs	High				PD
MSKCC11	p.E120*	High				PD
MSKCC12	p.D53fs	High				PR
MSKCC13	p.P173R	High	4.19	Probably damaging	1	PD
MSKCC14	p.A76fs	High				PD
MSKCC15	exon 3 splice variant	High				SD
MSKCC16	p.E33*	High				PD
MSKCC17	exon 2 splice variant	High				PD
MSKCC18	p.H174R	High	4.21	Probably damaging	1	PD
MSKCC19	p.Y60fs	High				PD
MSKCC20	p.K78*	High				PD
MSKCC21	p.Q159*	High				PD
MSKCC22	p.Q37*	High				PD
DFCI1	p.K84*	High				PD
DFCI2	p.A205fs	High				PD
DFCI3	p.G279fs	High				PR
DFCI4	p.R40fs	High				PD
DFCI5	p.A76P/Copy loss	Medium	3.365	Probably damaging	1	PD
DFCI6	c.464+1G>A	High				PD
DFCI7	p.G251V	Medium	3.15	Probably damaging	1	PD
DFCI8	p.E193D	Low	0.98	Probably damaging	0.962	PD
DFCI9	p.L245P	High	4.075	Probably damaging	1	SD
DFCI10	Copy loss	NA				PD
DFCI11	Copy loss	NA				PD
DFCI12	Copy loss	NA				PD
DFCI13	Copy loss	NA				PD
MGH1	p.G242V	High	4.69	Probably damaging	1	SD
MGH2	p.W308L	Medium	2.235	Probably damaging	1	PD
MGH3	p.G58Vfs*103	High				SD
MGH4	p.W308L, p.R384Q	Medium/Low	2.235/1.355	Probably damaging/benign	1/0.002	SD
MGH5	p.H174R	High	4.21	Probably damaging	1	PD
MGH6	Splice acceptor site	High				SD
MGH7	p.P323Yfs*13; SA site	High				PD
MGH8	p.D53Tfs*11	High				PD
CM057.1	p.Q214*	High				PD
CM057.2	p.D53Tfs*11	High				PD
CM057.3	p.W308C	Medium	2.785	Probably damaging	1	SD
CM057.4	p.P281Rfs*6	High				PD
CM057.5	splice site variant	High				PD
CM057.6	splice site variant	High				PD

Figure S2. Functional assessment of individual *STK11/LKB1* genomic alterations in the SU2C and CM-057 cohorts. Frameshift, nonsense and splice-site mutations were considered pathogenic. The functional significance of missense mutations was evaluated using a) Mutation Assessor (mutationassessor.org) and b) Polyphen-2. The overwhelming majority of identified *STK11/LKB1* alterations were predicted to be deleterious.

Figure S3

	STK11/LKB1 mutation	STK11/LKB1 IHC score	TMB (per Mb)	PD-L1 expression	KRAS mutation	Other co-mutations
MDACC2	p.L183P	NA	NA	NA	p.G13C	None detected
MSKCC3	X245_splice	NA	8.49	NA	p.G12C	INPP4B X45_splice KEAP1 p.S431F KMT2D p.G4716W MAP3K1 p.G530V E2F3 p.A159S TGFBR1 p.E247V MED12 p.M1473I
MSKCC12	p.D53Gfs*110	0	5.66	1%	p.G12C	FLT1 p.G82V DOT1L p.S490P KEAP1 p.V132G AURKA p.Q55L
DFCI3	p. P281Afs*6	NA	NA	0%	p.G12A	ATM p.Y2437D BMPR1A p.YQLPY453del TET2 p.K655fs High copy number gain: MYCL, MPL Low copy number gain: MCL1, CRTC2, NTRK1, SDHC, DDR2, RFWD2, CDC73, PIK3C2B, MDM4, H3F3A, FH, AKT3, GLI2, ERCC3, NFE2L2, PMS1, SF3B1, IDH1, ERBB4, CADM2, MECOM, ETV5, FANCE, CDKN1A, PIM1, CCND3, PRKDC, MYBL1, NBN, RAD21, EXT1, MYC, PTK2, RECQL4, PRF1, BMPR1A, PTEN, FAS, SUFU, SMC3, TCF7L2, FGFR2, SETBP1, SMAD2, SMAD4, BCL2 Single copy deletion: STK11, TCF3, GNA11, KEAP1, SMARCA4, BRD4, GATA4, WRN, FGFR1

Figure S3. Molecular characteristics of rare KL tumors in the SU2C cohort that responded to PD-1 blockade. The specific mutations in *STK11/LKB1* and *KRAS* are shown as well as the full panel of detected co-occurring genetic alterations. Where available, TMB (per Mb), STK11/LKB1 IHC score and tumor cell PD-L1 expression (as percent of positive staining membranes) are also indicated.

Figure S4

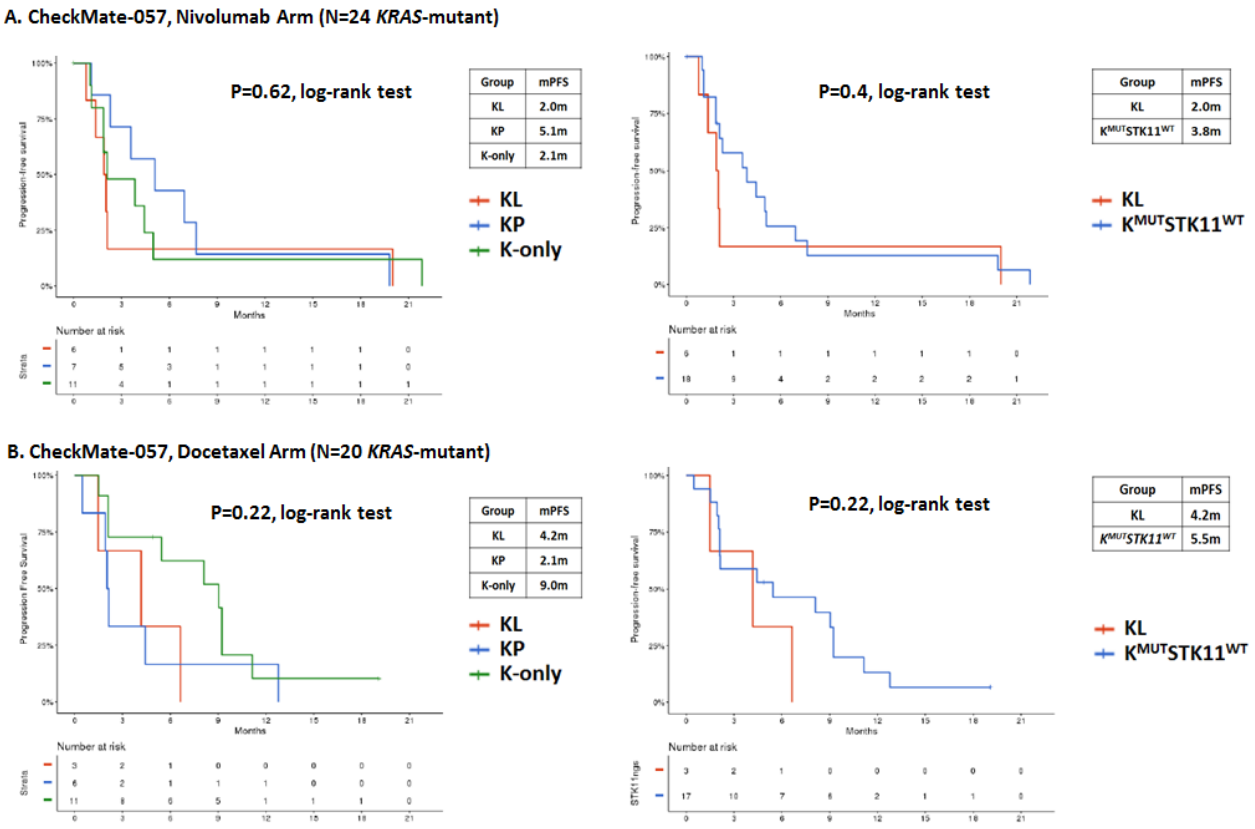

Figure S4. Progression-free survival in co-mutation defined subgroups of *KRAS*-mutant NSCLC in the Nivolumab (A) and Docetaxel (B) arms of CheckMate-057.

Figure S5

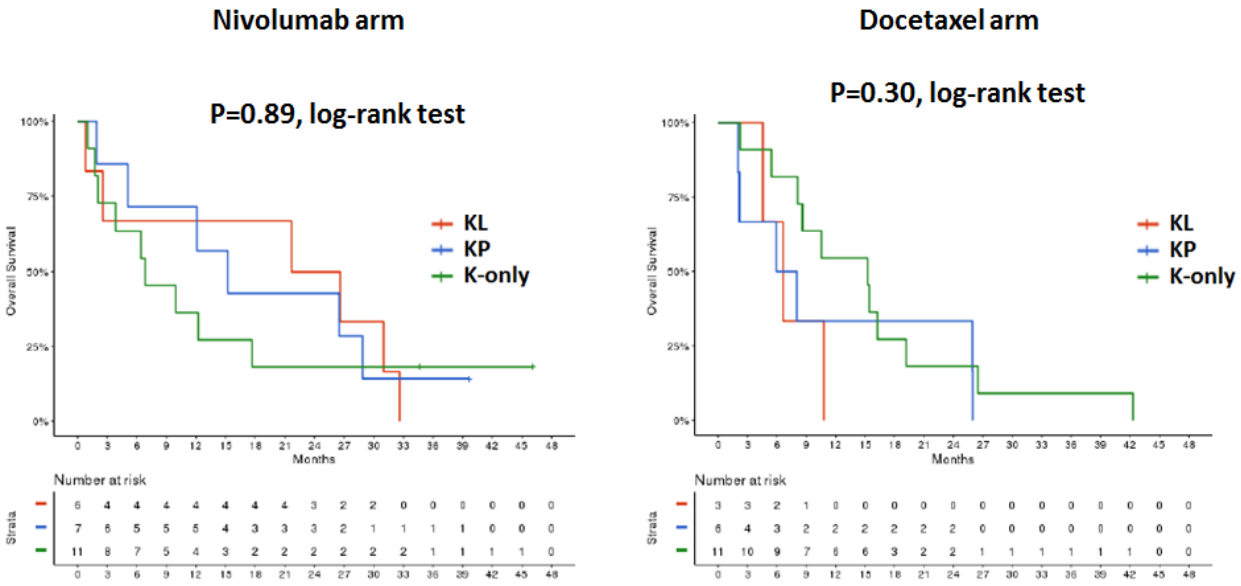

Figure S5. Overall survival with nivolumab and docetaxel in the KL, KP and K-only subgroups in CheckMate-057

Figure S6.

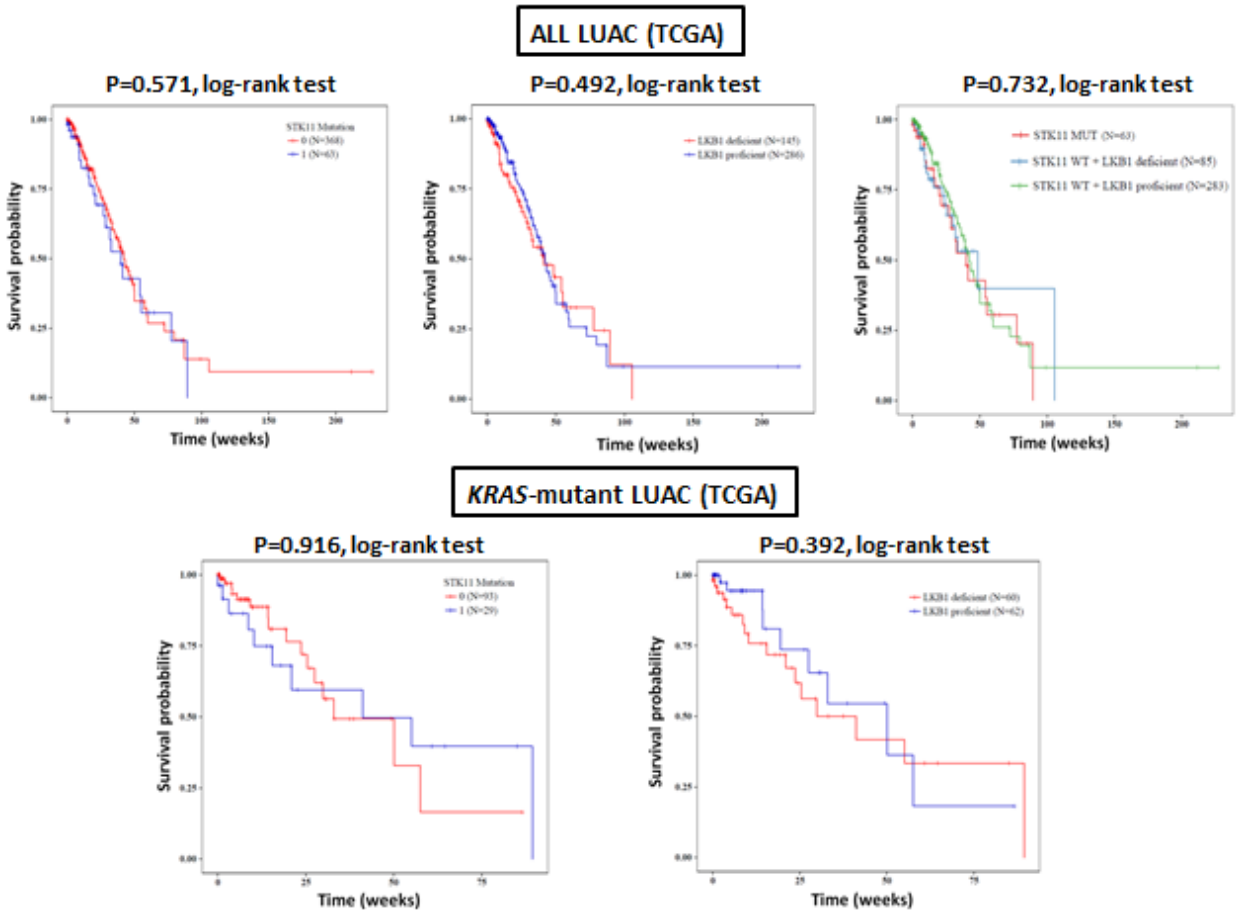

Figure S6. *STK11/LKB1* mutation or deficiency does not impact overall survival in the TCGA cohort of LUAC (N=431) and *KRAS*-mutant LUAC (N=122).

Figure S7.

A.

Characteristic	KL (N = 78)	KP (N = 160)	K-only (N = 108)	L (N = 77)	P (N = 344)	pan-WT (N = 157)
Age at sample procurement - yr						
Median	65	66	69	68	67	67
Range	46-83	43-85	39-87	39-87	32-88	23-88
Sex - no. of patients (%)						
Female	44 (56)	103 (64)	64 (59)	35 (45)	173 (50)	92 (59)
Male	34 (44)	57 (36)	44 (41)	42 (55)	171 (50)	65 (41)

B.

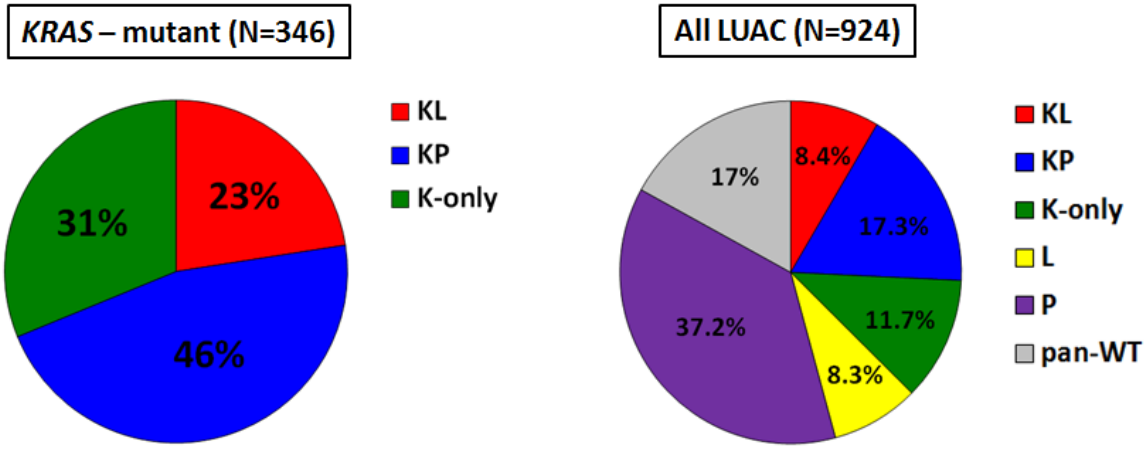

Figure S7. Demographic and molecular characteristics of 924 LUAC in the FM cohort. A. Baseline characteristics of the different genomic-alteration-defined subgroups. B. Fractional representation of the KL, KP, K-only subgroups among 346 *KRAS*-mutant LUAC. C. Pie chart representation of the relative frequencies of the KL, KP, K-only subgroups and their *KRAS*-wild-type counterparts (L – *STK11/LKB1* altered, P – *TP53* altered, pan-WT – no alteration in *KRAS*, *STK11/LKB1*, or *TP53*). *STK11/LKB1;TP53* double-mutant tumors with wild-type *KRAS* were classified as L.

Figure S8.

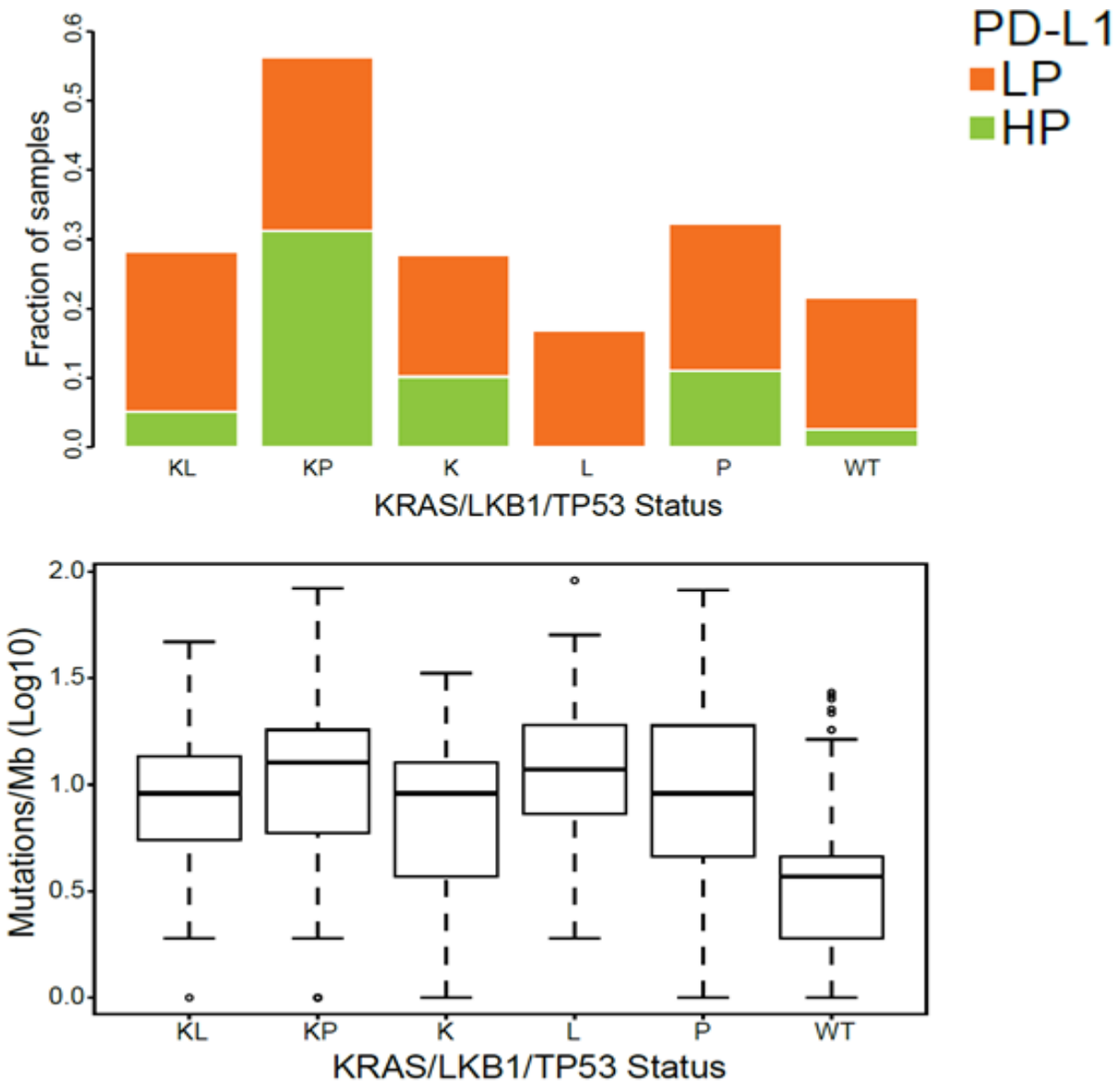

Figure S8. PD-L1 expression (top panel) and TMB (log10) (bottom panel) stratified by *STK11/TP53/KRAS* alteration in LUAC. For *KRAS*-wild-type samples: L – *STK11/LKB1* altered, P – *TP53* altered, WT – no alteration in *KRAS*, *STK11/LKB1*, or *TP53*. Note that L tumors (*STK11/LKB1*-altered with wild-type *KRAS*) also express low levels of PD-L1, despite high TMB that is comparable to that of KP tumors.

Figure S9.

A. FM cohort (N=346)

Group	PD-L1 expression (SP142)		
	0%	1%-49%	≥50%
KL	71.8% (56/78)	23.1% (18/78)	5.1% (4/78)
KP	43.7% (70/160)	25% (40/160)	31.3% (50/160)
K-only	72.2% (78/108)	17.6% (19/108)	10.2% (11/108)

P<0.001, Chi square test

B. SU2C cohort (N=69)

Group	PD-L1 expression (E1L3N)		
	0%	1%-49%	≥50%
KL	86.4% (19/22)	13.6% (3/22)	0% (0/22)
KP	45.5% (10/22)	31.8% (7/22)	22.7% (5/22)
K-only	68% (17/25)	16% (4/25)	16% (4/25)

P=0.018, Fisher's exact test

C. CM-057 cohort (N=44)

Group	PD-L1 expression (28.8)		
	0%	1%-49%	≥50%
KL	88.9% (8/9)	11.1% (1/9)	0% (0/9)
KP	15.4% (2/13)	30.8% (4/13)	53.8% (7/13)
K-only	31.8% (7/22)	27.3% (6/22)	40.9% (9/22)

P=0.0014, Fisher's exact test

Figure S9. Tumor-cell membranous expression of PD-L1 in the KL, KP and K-only subgroups across the FM, SU2C and CM-057 clinical cohorts. All patients (N=44) regardless of treatment arm allocation from CM-057 were included in the analysis. A two-tailed Chi square or Fisher's exact test (computed from a 2x3 contingency table) was used to assess the significance of the association between group membership and PD-L1 expression status [PD-L1 negative (0%) or PD-L1 positive (≥1%)].

Figure S10.

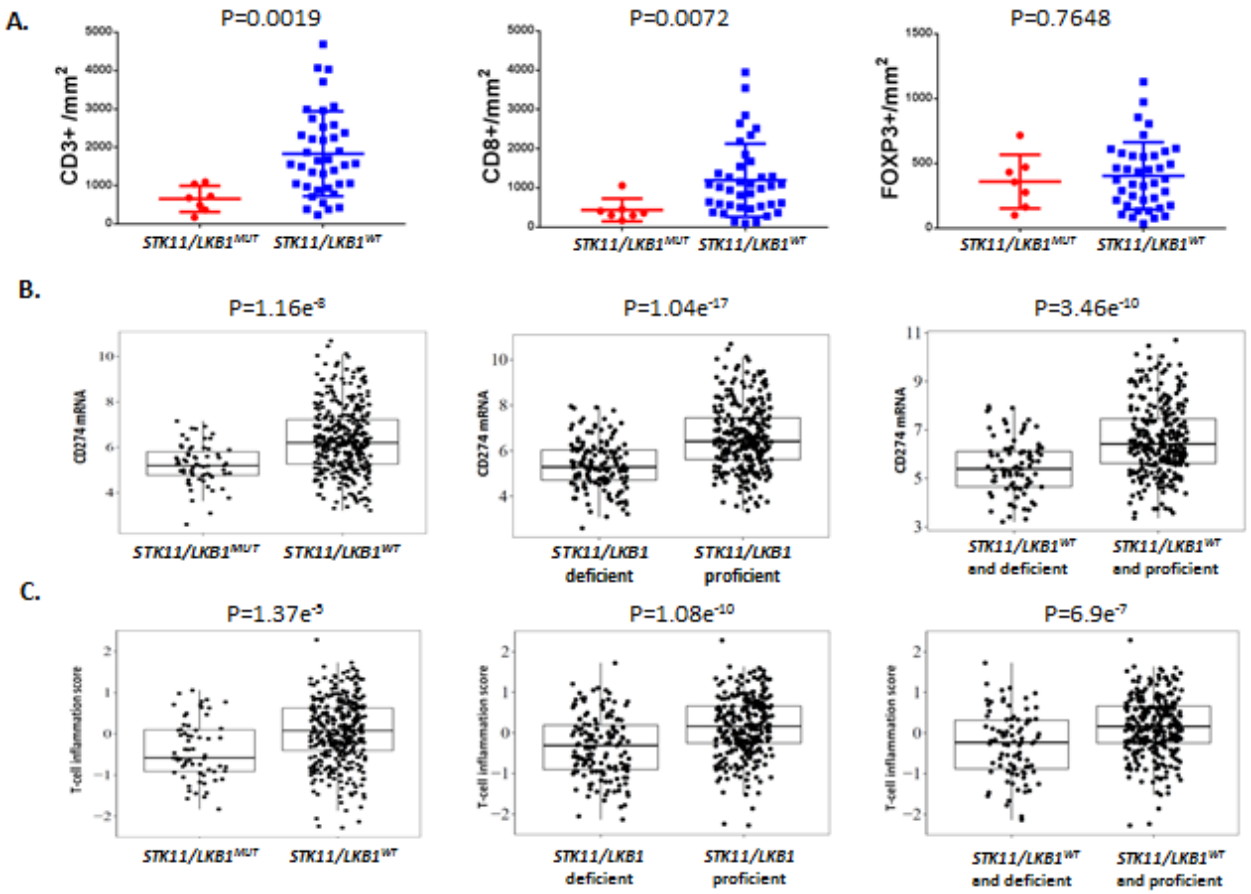

Figure S10. STK11/LKB1 inactivation is associated with a non-T-cell-inflamed tumor immune microenvironment in lung adenocarcinoma. A. Densities of infiltrating CD3+, CD8+ and FOXP3+ T-lymphocytes in *STK11/LKB1*-mutant and wild-type LUAC (regardless of *KRAS* status) from the PROSPECT cohort of surgically resected, early-stage LUAC. The Mann-Whitney U test was used to compare densities of TILs between *STK11/LKB1*-mutant and wild-type tumors. P≤0.05 was considered statistically significant. B. Comparison of *CD274 (PD-L1)* mRNA levels (log2 transformed RSEM values) (from RNASeq data, downloaded from the TCGA website on 08/26/2016) between *STK11/LKB1*-mutant and wild type (left panel) or STK11/LKB1 deficient and proficient (middle panel) LUAC in the TCGA cohort. STK11/LKB1 deficiency was determined using a previously validated gene expression signature. The right panel depicts *CD274* mRNA levels (log2 transformed RSEM values) in STK11/LKB1 deficient LUAC with wild-

type *STK11/LKB1* status compared to STK11/LKB1 proficient wild-type tumors. Student's t-test was used for statistical comparisons. C. *STK11/LKB1*-altered or deficient LUAC exhibit lower levels of T-cell signature transcripts (from a previously established 13-gene signature) (30).

Figure S11.

A. Progression-free survival

	loglik	Chisq	df	p-value
Null model	-107.38			
PD-L1	-107.36	0.0356	1	0.850374
STK11	-102.08	10.5654	1	0.001152
PD-L1 STK11 interaction	-102.08	0.4896	1	0.484087

PD-L1 ≥ 50% group:
HR 0.14 (95% CI, 0.04 - 0.5), P= 0.0005, log-rank test

PD-L1 <50% group:
HR 0.27 (95% CI, 0.08 - 0.94), P=0.0278, log-rank test

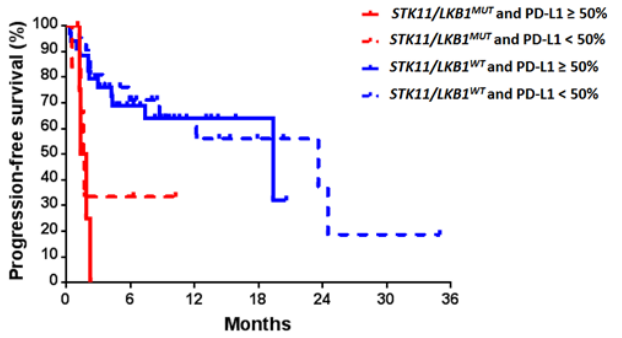

B. Overall survival

	loglik	Chisq	df	p-value
Null model	-36.765			
PD-L1	-36.765	0.0515	1	0.8204261
STK11	-30.502	12.5266	1	0.0004012
PD-L1 STK11 interaction	-30.358	0.2883	1	0.5913080

PD-L1 ≥ 50% group:
HR 0.11 (95% CI, 0.015 - 0.78), P= 0.0075, log-rank test

PD-L1 <50% group:
HR 0.05 (95% CI, 0.004 - 0.49), P=0.0278, log-rank test

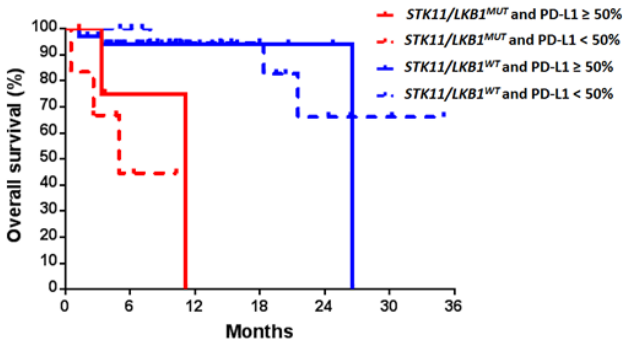

Figure S11. *STK11/LKB1* genomic alterations impact PFS and OS with PD-1/PD-L1 blockade independently of the level of PD-L1 expression in PD-L1 positive NSCLC. A. (Left panel) Analysis of the deviance table for PFS. The interaction effect is not significant (P=0.48), indicating that the effect of *STK11/LKB1* genomic alterations on PFS does not differ significantly across the two PD-L1 expression groups (≥ 50% and <50%). (Right panel) Kaplan-Meier estimates of PFS with PD-1/PD-L1 blockade in *STK11/LKB1*-mutant and wild-type groups depending on PD-L1 expression. B. (Left panel) Analysis of the deviance table for OS. The interaction effect is not significant (P=0.59), indicating that the effect of *STK11/LKB1* genomic alterations on OS does not differ significantly across the two PD-L1 expression groups (≥ 50% and <50%). (Right panel) Kaplan-Meier estimates of OSS with PD-1/PD-L1 blockade in *STK11/LKB1*-mutant and wild-type groups depending on PD-L1 expression.

Figure S12.

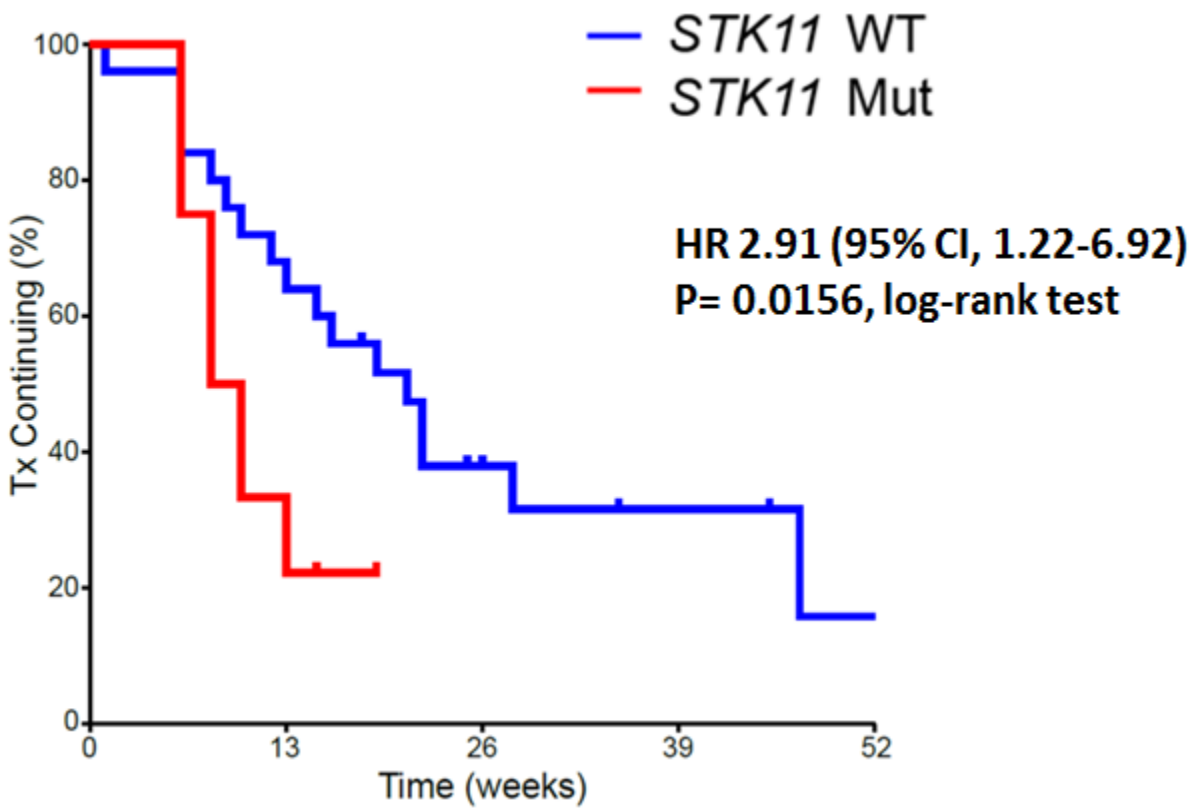

Figure S10. *STK11/LKB1* genomic alterations are associated with shorter time on PD-1/PD-L1 inhibitor in non-squamous NSCLC with intermediate/high TMB. Kaplan-Meier estimates of time to treatment discontinuation in a separate cohort of 81 patients with non-squamous NSCLC treated with anti-PD(L)-1 therapy (68 nivolumab, 6 pembrolizumab, 5 avelumab, 1 atezolizumab, 1 durvalumab).

Figure S13.

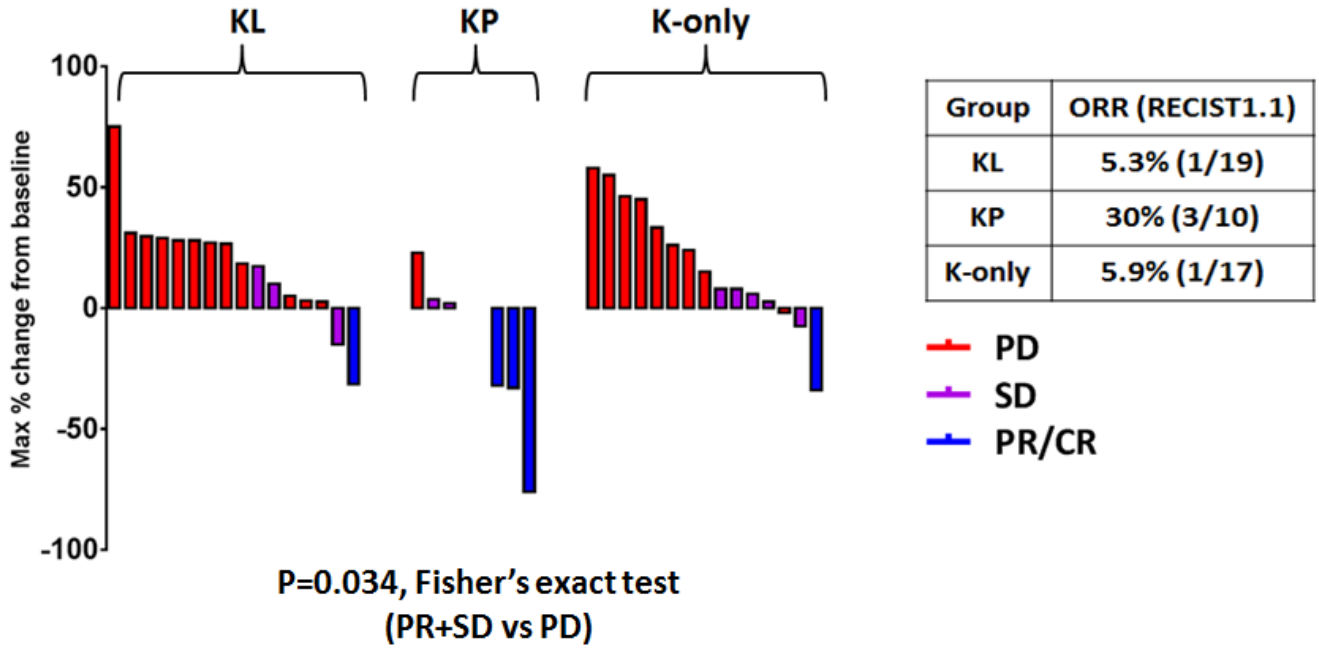

Group	ORR (RECIST1.1)
KL	5.3% (1/19)
KP	30% (3/10)
K-only	5.9% (1/17)

Figure S13. *TP53* genomic alterations may aid prediction of PD-1 inhibitor response in PD-L1-negative *KRAS*-mutant LUAC. Disease control rate with PD-1 blockade among PD-L1-negative *KRAS*-mutant LUAC differs significantly between KP, KL and K-only subgroups (Left panel). Waterfall plot demonstrating patient-level maximal % change in tumor burden from baseline in response to PD-1/PD-L1 inhibitor therapy in PD-L1-negative *KRAS*-mutant LUAC. Fisher's exact test (2x3 contingency table) was used to assess the significance of the association between co-mutation group membership and disease control rate (CR/PR/SD vs PD). Among PD-L1-negative LUAC, KP exhibited the highest DCR (70%) with PD-1 blockade with PR observed in 3/10 (Right panel).

Figure S14.

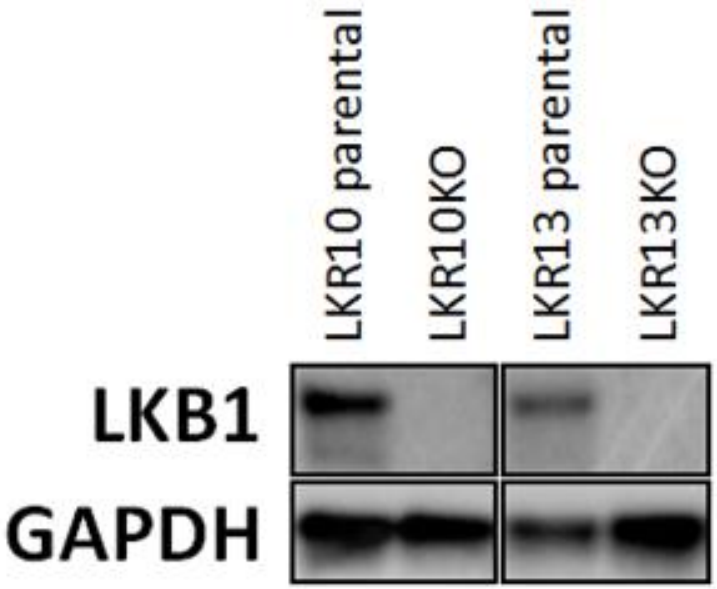

Figure S14. LKB1 expression in isogenic derivatives of the LKR10 and LKR13 *Kras*-mutant murine LUAC cell line with CRISPR/Cas9-mediated *Stk11/Lkb1* knockout. Immunoblotting using a commercially available validated rabbit monoclonal antibody (clone D60C5, Cell Signaling Technology) confirms efficient depletion of LKB1 in single-cell derived LKR10KO and LKR13KO lines.

Figure S15.

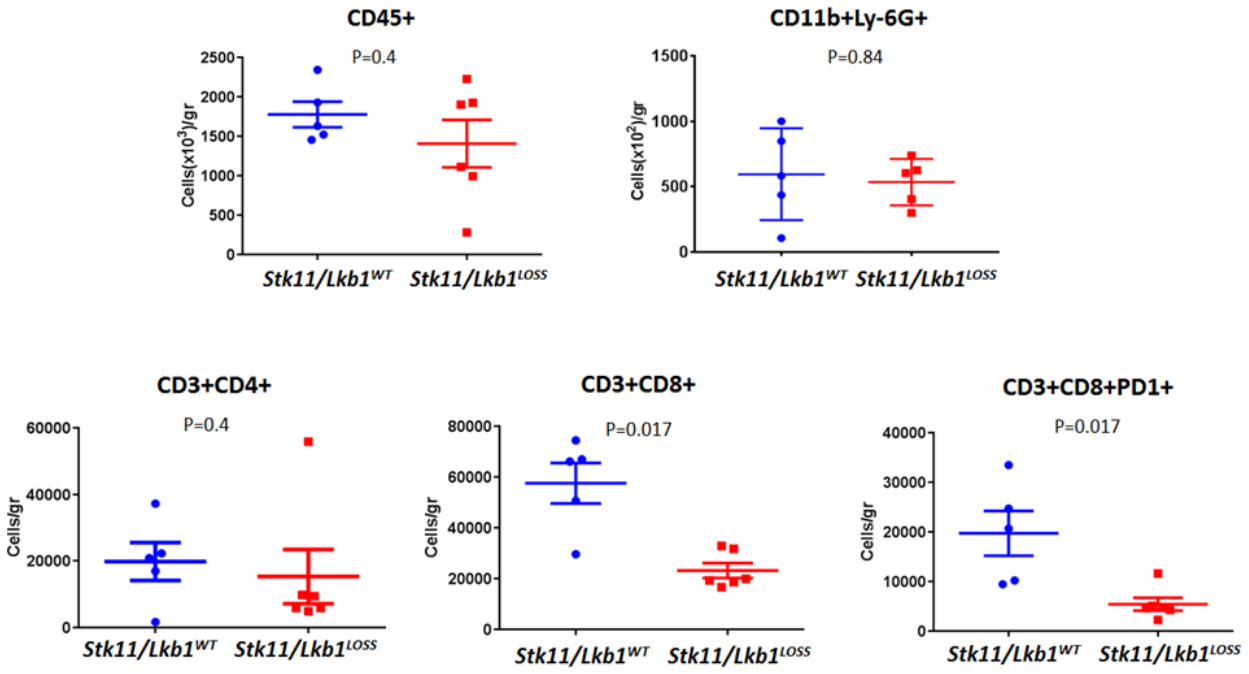

Figure S15. *Stk11/Lkb1* genetic ablation directly promotes establishment of a "cold" tumor immune microenvironment in a syngeneic murine model of *Kras*-mutant LUAC (LKR13). Numbers of CD45+ (top left panel), CD11b+Ly-6G+ (top right panel), CD3+CD4+ (bottom left panel), CD3+CD8+ (bottom middle panel) and CD3+CD8+PD1+ (bottom right panel) per gr of explanted subcutaneous tumors, following dissociation to a single cell suspension and FACS sorting. The Mann Whitney U test was used to compare numbers of the indicated cellular populations per gr of excised whole tumor. P≤0.05 was considered statistically significant.